NeuroToxicology 49 (2015) 8–14

Contents lists available at ScienceDirect

NeuroToxicology

Ex vivo magnetic resonance imaging in South African manganese mine workers

Susan R. Criswell [a,*], Gill Nelson [b], Luis F. Gonzalez-Cuyar [c], John Huang [d], Joshua S. Shimony [e], Harvey Checkoway [f], Christopher D. Simpson [g], Russell Dills [g], Noah S. Seixas [g], Brad A. Racette [a,b]

[a] Department of Neurology, Washington University School of Medicine, 660 South Euclid Ave., Box 8111, St. Louis, MO 63110, USA
[b] School of Public Health, Faculty of Health Sciences, University of the Witwatersrand, 27 St Andrews Rd, Parktown 2193, South Africa
[c] Department of Pathology, University of Washington, UW Medicine Pathology, Box 357470, Seattle, WA 98195-7470, USA
[d] Program in Physical Therapy, Washington University School of Medicine, 4444 Forest Park Ave., Suite 1101, Box 8502, St. Louis, MO 63108, USA
[e] Department of Radiology, Washington University School of Medicine, 660 South Euclid Ave., Box 8131, St. Louis, MO 63110, USA
[f] Department of Family Medicine and Public Health, UC San Diego School of Medicine, 9500 Gilman Drive-0628, La Jolla, CA 92093-0628, USA
[g] Department of Environmental and Occupational Health Sciences, University of Washington, School of Public Health Box 357234, Seattle, WA 98195-7234, USA

ARTICLE INFO

Article history:
Received 26 November 2014
Accepted 13 April 2015
Available online 23 April 2015

Keywords:
Manganese
Ex vivo
MRI
Miners

ABSTRACT

Background: Manganese (Mn) exposure is associated with increased T1-weighted magnetic resonance imaging (MRI) signal in the basal ganglia. T1 signal intensity has been correlated with occupational Mn exposure but not with clinical symptomatology or neuropathology.
Objectives: This study investigated predictors of ex vivo T1 MRI basal ganglia signal intensity in neuropathologic tissue obtained from deceased South African mine workers.
Methods: A 3.0 T MRI was performed on ex vivo brain tissue obtained from 19 Mn mine workers and 10 race- and sex-matched mine workers of other commodities. Basal ganglia regions of interest were identified for each subject with T1-weighted intensity indices generated for each region. In a pathology subset, regional T1 indices were compared to neuronal and glial cell density and tissue metal concentrations.
Results: Intensity indices were higher in Mn mine workers than non-Mn mine workers for the globus pallidus, caudate, anterior putamen, and posterior putamen with the highest values in subjects with the longest cumulative Mn exposure. Intensity indices were inversely correlated with the neuronal cell density in the caudate ($p = 0.040$) and putamen ($p = 0.050$). Tissue Mn concentrations were similar in Mn and non-Mn mine workers. Tissue iron (Fe) concentration trended lower across all regions in Mn mine workers.
Conclusions: Mn mine workers demonstrated elevated basal ganglia T1 indices when compared to non-Mn mine workers. Predictors of ex vivo T1 MRI signal intensity in Mn mine workers include duration of Mn exposure and neuronal density.

1. Introduction

Occupational Mn exposure is associated with parkinsonism (Racette et al., 2012), cognitive dysfunction (Bowler et al., 2007; Park et al., 2009; Rodier, 1955), and increased signal on T1-weighted magnetic resonance imaging (MRI) in the basal ganglia (Criswell et al., 2012; Huang, 2007; Kim et al., 1999; Nelson et al., 1993). The signal changes are presumed to be caused by Mn deposition and its secondary effects on the magnetic resonance properties of surrounding brain tissue (Newland, 1999; Kang et al., 1984). The intensity of in vivo pallidal signal correlates with Mn exposure (Dietz et al., 2001) and Mn blood levels (Chang et al., 2010) but the relationship with clinical symptomatology has not been clearly established. Moreover, the relationship between Mn tissue concentration and neuropathology has been inconsistent. Previous studies with subcutaneous manganese oxide exposure in monkeys resulted

* Corresponding author at: Washington University School of Medicine, 660 South Euclid Ave., Box 8111, St. Louis, MO 63110, USA. Tel.: +1 314 362 7272; fax: +1 314 747 3274.
E-mail address: criswells@neuro.wustl.edu (S.R. Criswell).

http://dx.doi.org/10.1016/j.neuro.2015.04.002
0161-813X/

in severe loss of pallidal nerve cells and astrogliosis with increased regional Mn deposition (Eriksson et al., 1987). However, rhesus monkeys injected with manganese chloride developed similar findings of pallidal and nigral gliosis with astrocytosis, but no change in tissue Mn (Olanow et al., 1996). More recently, elevated Mn tissue concentrations have been reported throughout the basal ganglia of Mn-injected macaques, but post-mortem immunohistochemistry results were normal (Guilarte et al., 2006, 2008).

Pathologic studies in occupationally-exposed humans are very limited but similarly inconsistent. Autopsy data from a 52-year-old man exposed to Mn in an ore plant describe pallidal cell loss but normal tissue Mn concentration (Yamada et al., 1986). Older reports document cell loss in the putamen and pallidum but did not examine Mn tissue concentrations (Canavan et al., 1934; Casamajor, 1913). All of these human studies in occupationally-exposed subjects predate modern immunohistochemical studies, and none have corresponding imaging. Further evaluation of the relationship between imaging characteristics and neuropathology could provide valuable information on the mechanism of Mn neurotoxicity and a better understanding of the clinical significance associated with the increased T1 signal characteristic of this exposure.

Ex vivo MRI imaging permits correlation of histopathology with MRI signal intensity (Augustinack et al., 2013; Baltes et al., 2011; Garbelli et al., 2011; Riddle et al., 2011). Ex vivo imaging also provides a cost effective method of establishing imaging parameters for future in vivo sequences as these scans can be completed at a fraction of the cost and with no risk to human subjects. However, formalin fixed ex vivo tissue has different physical properties than in vivo tissue and subsequently different T1 imaging properties (Baba et al., 1994; Henriksen et al., 1993; Tovi and Ericsson, 1992). Therefore, the primary objective of this study was to validate the use of ex vivo imaging in Mn neurotoxicity by confirming T1 signal differences persist post-mortem in Mn-exposed subjects. Our secondary objective was to explore the relationships between ex vivo T1 imaging, neuropathology, and tissue metal concentration using post-mortem brain tissue from South African Mn mine workers and matched non-Mn mine workers.

2. Methods

2.1. Brain acquisition

This study was approved by the Washington University Human Research Protection Organization and the University of the Witwatersrand Human Research Ethics Committee. Race- and sex-matched Mn mine workers and non-Mn mine workers were selected from our previously established autopsy program (Nelson et al., 2012) for imaging and analysis. Upon notification of the death of a mine worker, consent was obtained from the next-of-kin. The brain specimens were suspended in 10% neutral buffered formalin for a minimum of three weeks, after which they were shipped to Washington University for ex vivo MRI imaging, and then to the University of Washington for pathology and tissue metal analysis.

2.2. Exposure assessment

After obtaining consent, an occupational health nurse interviewed the family to obtain occupational and medical histories. Permission to access the deceased subject's medical and employment records was also requested to verify accuracy of the historical information. Workers whose medical histories indicated any neurologic diagnosis were excluded. An industrial hygienist reviewed the occupational history and employment records and assigned duration of Mn exposure to each subject.

2.3. MRI studies

Fixed brains were placed in the scanner within MRI compatible, plastic containers filled with 10% formaldehyde solution with plastic supports to prevent movement. Imaging was performed on a 3.0 T Siemens Trio scanner (Erlangen, Germany). A Siemens adapted neuromelanin imaging technique (Astafiev et al., 2010) (repetition time = 600 ms, echo time = 14 ms, flip angle = 120°, voxel dimensions 0.7 mm × 0.43 mm × 2.5 mm, matrix dimensions 314 × 550, 11 axial slices) was used to obtain high-resolution T1-weighted images through the basal ganglia and midbrain. A transverse slice through a Mn miner brain demonstrates the differences in T1 weighted signal from fixed tissue including the including the gray matter to white matter signal reversal that occurs at 11 weeks post fixation (Tovi and Ericsson, 1992) (Fig. 1). A single reviewer, blinded to the clinical status of the subject, outlined volumes of interest (VOIs) including the caudate, globus pallidus, anterior and posterior putamen, and standardized white matter regions on individual images. The intensity of the signal on the T1-weighted image in the VOI was compared by calculating an intensity index for each region in each subject. The regional intensity indices were defined as the ratio of T1 signal in the VOI to a standard frontal white matter reference region following previously used methods for the pallidal index (Spahr et al., 1996).

$$\text{Intensity index} = \frac{\text{VOI}}{\text{Left white matter control region} + \text{Right white matter control region}} \times 100$$

Intensity indices were created for the globus pallidus, caudate, anterior putamen, and posterior putamen using the same reference control regions. A combined basal ganglia intensity index was created by averaging the intensity indices of all four VOIs.

All brains were scanned on the same scanner in the same configuration and with the same pulse sequence. The intensity indices as ratios should thus be largely independent of any underlying signal inhomogeneity. To confirm this, we compared white matter signal intensity in the control region (the denominator of the intensity indices) across all subjects (mean = 926.26, standard deviation 80.04) which corresponded to a very low coefficient of variation of 8.64% with <2% difference between Mn miner workers and non-Mn mine workers.

2.4. Neuropathology

A board certified neuropathologist performed a gross examination. The cerebrum and posterior fossa contents were embedded in a 3% agar solution and sliced coronally and axially, at 4 mm intervals respectively. Formalin fixed paraffin embedded (FFPE) tissue blocks were sectioned and deparaffinized rehydrated slides were stained with hematoxylin and eosin. Automated immunohistochemistry was performed on tissue sections from the basal ganglia using mouse monoclonal antibodies for glial fibrillary acidic protein (GFAP) (Dako, USA) to label astrocytes, microtubule associated protein-2 (MAP-2) (Millipore, USA) to label neurons, and CD68 (Dako, USA) to label macrophages and microglia using a Leica Bond III fully automated immunohistochemistry and in situ hybridization staining system (Leica Bio-Systems, USA). FFPE tissue blocks corresponding to a unilateral coronal section of the

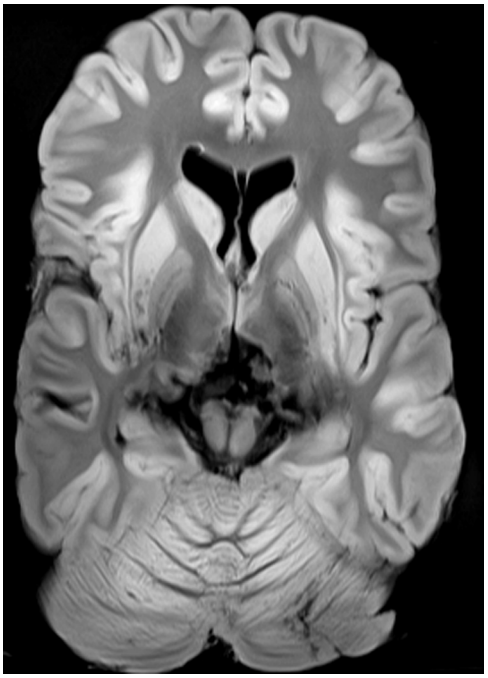

Fig. 1. High-resolution T1 basal ganglia imaging from a formalin fixed Mn mine worker brain.

corpus striatum were selected. The regions of interest: caudate, putamen, and globus pallidus (globus pallidus externus and globus pallidus interna were combined for statistical analysis) were delineated on the glass slides. Strict histological criteria and immunohistochemistry were used to count the different cell types, on a light microscope (Olympus, Japan), per 40× objective as previously described (Gonzalez-Cuyar et al., 2013).

2.5. Metal quantification

Tissue for metal quantification was acquired from formalin fixed non-paraffin embedded coronal sections of corpus striatum (4 mm thick) from an area adjacent to the block where cell density studies were performed. An aliquot of approximately 50 mg of tissue was obtained from each tissue sample and analyzed based on Environmental Protection Agency method 3052 and Yoo et al. (2002) using open-vessel microwave-assisted digestion (CEM Mars Xpress) in polypropylene centrifuge tubes and diluted nitric acid (0.5 mL; trace-metals grade, Fisher; 50:50 v/v with 18 MΩ deionized water, Barnstead Nanopure) containing 50 ng/mL terbium recovery standard. The digested samples were brought to 2 mL prior to analysis by ICP-MS. Dilutions in 10% nitric acid were made as necessary to stay within calibration range. Elements of interest were acquired in He-mode on an Agilent 7500-CE ICPMS and CETAC ASX-510 autosampler. Internal standards (scandium, ytterbium and iridium at 10 μg/mL) were added to the sample flow from the autosampler by peristaltic pump. Scandium was used as the internal standard for Mn, whereas ytterbium was used for Fe. Calibrants were diluted in 10% nitric acid of certified reference materials (Aristar BDH) and verified against a second source (Ultra Scientific). Results were corrected for process blank and terbium recovery. Assay accuracy and precision was established by replicate analysis of standard reference material oyster tissue SRM 1566b (NIST, Gaithersburg, MD) and were determined to be 96 ± 3% for Mn and 86 ± 4% for Fe. The limit of quantification, assuming 50 mg of tissue, was 0.002 ng/mg for Mn and 0.06 ng/mg for Fe.

2.6. Statistical analysis

Demographic variables were compared between the Mn and non-Mn mine workers using a Mann–Whitney *U* test. Multivariate generalized linear modeling (GLM) was performed to compare differences between groups for each regional index (right and left side averaged). The Benjamini and Hochberg false discovery rate (FDR) correction was used to correct for multiple comparisons with FDR = 0.05 (Benjamini and Hochberg, 1995). The model was adjusted for covariates reported to affect in vivo or post-mortem T1 signal including age of death, time from the last mining exposure to scan, and the death to scan interval (Tovi and Ericsson, 1992; Salat et al., 2009). Years from last mining exposure was included since T1 signal intensity in subjects with Mn toxicity secondary to liver failure have been reported to normalize post-transplantation (Maffeo et al., 2014; Pujol et al., 1993). To further investigate the relationship between intensity indices and exposure, we categorized cumulative years worked in mines into low (<5 years) and high (≥5 years) exposed groups. Five years of Mn exposure was the cutoff value at which there were a sufficient number of subjects to maintain the model. As this choice was made post hoc, we repeated the analysis with the Mn group tertiled into exposure groups. Multivariate GLM was used to examine differences in regional tissue Mn and Fe concentrations between exposed and non-exposed groups for each region adjusted for the time from last Mn exposure to death. The relationships between ipsilateral intensity indices, tissue metals, and regional cell counts were examined using linear regression adjusting for age at death and the death to scan interval. Given the relatively smaller number of subjects with pathology and tissue Mn concentrations, we did not attempt to correct for multiple comparisons in these analyses. The statistical software SPSS for Windows v21.0 (Chicago, IL) was used for data analysis.

3. Results

We identified 28 deceased black male Mn mine workers and 13 deceased race- and sex-matched reference non-Mn mine workers for this study. Of the subjects identified, three Mn-exposed brains and one non-exposed brain were not of sufficient quality for imaging. In addition, six Mn mine workers and two non-Mn mine workers lacked sufficient demographic or exposure data. The remaining 19 Mn mine workers were compared with 10 race- and sex-matched non-Mn mine workers. Demographics for the two groups are presented in Table 1. Mn mine workers were slightly younger than non-Mn mine workers, had greater cumulative exposure to mining, and died earlier relative to their last mining exposures. Some of the Mn mine workers also had lesser exposures to other mining commodities; therefore, cumulative exposures to all commodities as well as Mn-specific exposures are included in Table 1.

Intensity indices were higher in the Mn mine workers compared to the non-Mn mine workers across the caudate ($p = 0.05$), globus pallidus ($p = 0.016$), anterior putamen ($p = 0.006$), posterior putamen ($p = 0.007$), and combined basal ganglia index ($p = 0.004$) (Fig. 2A). Within the Mn exposed group, Mn mine workers with longer duration of exposure had higher basal ganglia intensity indices. The pattern of increasing regional intensity indices across exposure groups and post hoc differences between the two Mn-exposed groups and the reference subjects are illustrated (Fig. 2B). The relationship between intensity indices and Mn exposure was consistent when we repeated the analysis with the Mn groups divided evenly into tertiles of exposure.

To better understand the predictors of basal ganglia MRI signal intensity, we investigated the relationship between intensity indices, regional cell density, and tissue Mn concentration in seven

Table 1
Demographics for all mine workers and the pathology subset.

Characteristic	All mine workers ($n=29$)			Pathology subset ($n=14$)		
	Non-Mn mine workers	Mn mine workers	p-Value	Non-Mn mine workers	Mn mine workers	p-Value
Age (mean ± SD)	58.22 ± 13.24	56.17 ± 7.7	0.623	58.36 ± 14.14	55.38 ± 8.54	0.643
Cumulative mining exposure – all mines (median years, IQR)	7.88 (1.8–18.17)	21.08 (12.36–31.09)	0.029*	12.00 (4.26–18.37)	21.08 (12.37–30.50)	0.012*
Cumulative Mn mining exposure (median years, IQR)	–	16.63 (4.31–31.71)	–	–	7.33 (1.3–24.9)	–
Mining employment to death (median years, IQR)	21.99 (13.80–33.40)	2.52 (0–18.11)	0.006*	18.67 (14.0–36.0)	0.73 (0–17.8)	0.041*
Death to autopsy (median days, IQR)	6.0 (3.75–7.25)	4.0 (3.0–6.0)	0.157	5.0 (3.0–6.0)	5.0 (3.0–6.0)	0.801
Death to scan (median days, IQR)	228 (203–255)	287 (157–316)	0.192	235 (221–254)	302 (284–477)	0.019*

Abbreviations: SD, standard deviation; IQR, interquartile range.
* Mann–Whitney U test compared Mn to non-Mn mine workers, $p \leq 0.05$.

Mn mine workers and seven non-Mn mine workers in whom detailed neuropathologic data were available (Gonzalez-Cuyar et al., 2013). The demographic characteristics of this subset are reported in Table 1. As in the entire dataset, T1 indices in this subset were higher in all regions in Mn mine workers than non-Mn mine workers. Linear regression demonstrated an inverse relationship between the MAP2 stain neurons and the signal intensity for the caudate and putamen but not the globus pallidus. There was also a trend toward increasing CD68 stained microglial cells with increasing T1 signal across all regions (Table 2).

Tissue metal analysis for the caudate, putamen, and globus pallidus was performed in 12 of the 14 subjects with neurohistochemical studies with sufficient tissue and analysis verification. There were no differences in tissue Mn between Mn and non-Mn mine workers. Tissue Fe was lower in the Mn mine workers across all regions sampled, but the differences were not statistically significant (Table 3). There was no relationship between regional tissue Mn and Fe with regional intensity indices, cell density, or Mn exposure. Similarly, there were no differences in tissue concentrations of potassium, phosphorus, calcium, copper, zinc, lead, and magnesium between Mn and non-Mn mine workers for all regions sampled.

4. Discussion

In this study, we demonstrated elevated MRI T1 intensity indices across the basal ganglia in ex vivo specimens from deceased Mn mine workers that increased with the duration of Mn exposure. These findings replicate previous in vivo studies of Mn exposure despite the differences between ex vivo and living tissue (Criswell et al., 2012; Kim et al., 1999; Dietz et al., 2001; Chang et al., 2010). We believe this provides compelling evidence for the validity of ex vivo imaging as a tool for evaluating the relationships between Mn exposure, MRI imaging characteristics, and pathology.

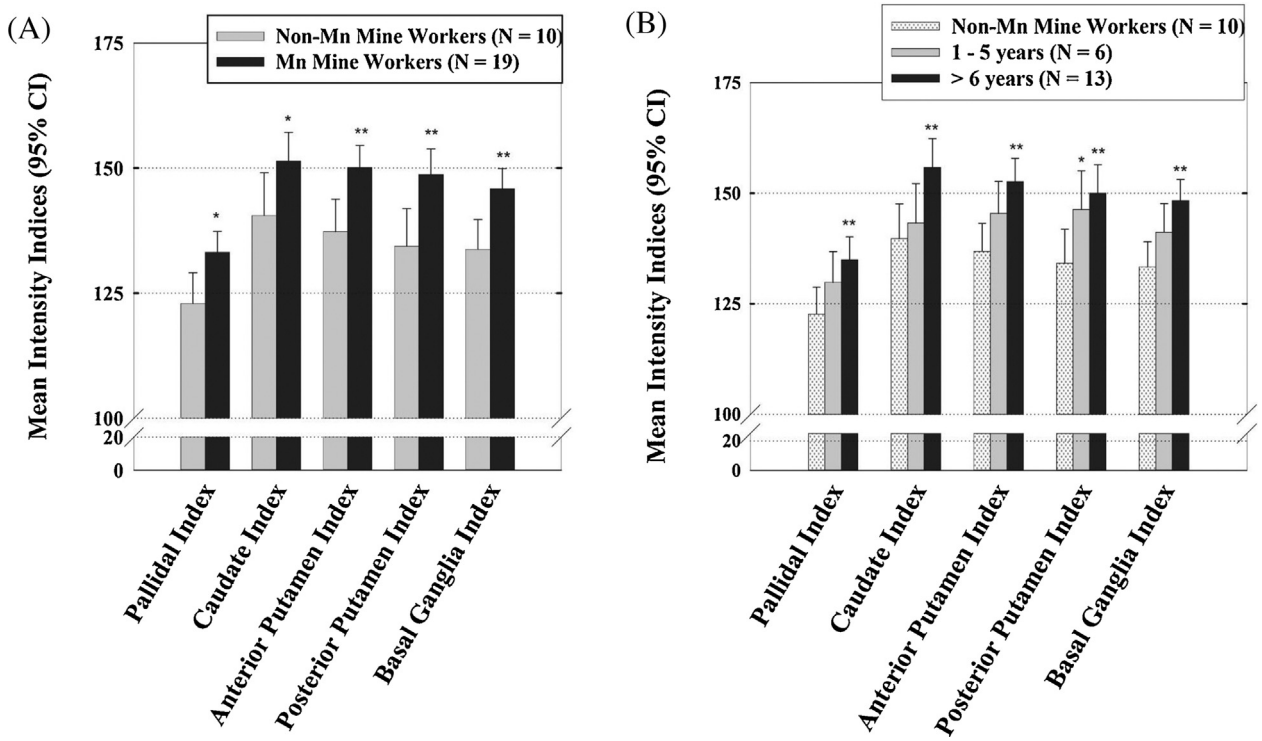

Fig. 2. T1 Intensity indices for each region in (A) Mn miners and non-Mn miners and (B) high- and low-exposed Mn miners and non-Mn miners adjusted for age of death, time from last Mn exposure, and the death to scan interval. *$p \leq 0.05$, **$p \leq 0.01$ when compared to reference non-Mn miners.

Table 2
T1 Indices and regional cell density ($n = 14$).

Average cells per HPF by Stain	Region	Caudate index		Putamen index		Pallidal index	
		Beta	p	Beta	p	Beta	p
GFAP	Caudate	0.433	0.162				
	Putamen			−0.176	0.600		
	Globus pallidus					0.376	0.211
CD68	Caudate	0.125	0.682				
	Putamen			0.372	0.238		
	Globus pallidus					0.379	0.274
MAP2	Caudate	−0.538	0.040*				
	Putamen			−0.564	0.050*		
	Globus pallidus					0.036	0.920

The relationships between ipsilateral intensity indices and regional cell counts were examined using linear regression adjusted for age and time from death to scan.
* $p \leq 0.05$.

We demonstrated a persistent elevation of the intensity indices despite relatively prolonged periods from the subjects' last Mn exposure to death (median 2.52, IQR 0–18.11 years). Previous reports indicate that T1 signal changes are potentially reversible as the interval from Mn exposure increases (Butterworth et al., 1995; Han et al., 2008). However, the findings from this ex vivo MRI study are consistent with a recent study in which some subjects with Mn toxicity secondary to liver failure had resolution of their pallidal T1 signal hyperintensities post-transplantation, while others had persistent signal changes at 24 months post-transplant (Maffeo et al., 2014). Mn-exposed non-human primates have also demonstrated similar sustained elevation in pallidal T1 signal up to 182 days post-exposure (duration of the experiment) (Newland, 1999). This reinforces that while the increased T1 signal intensity is potentially reversible, there appears to be a threshold at which the signal changes become permanent.

We were able to examine the relationships between ex vivo T1 imaging characteristics and neuropathology using cell density and tissue Mn concentrations in a subset of Mn- and non-Mn-exposed miners. While the sample is small, this study is the largest imaging/pathology correlation study conducted in Mn-exposed subjects. We found an inverse relationship between the T1 intensity indices and neuronal density in the caudate and putamen. This is intriguing given our recent study demonstrated lower caudate (14%) and putamen (8%) neuronal cell density in Mn mine workers compared to the non-Mn mine workers groups (Gonzalez-Cuyar et al., 2013). In addition, there was a direct relationship, although not statistically significant, between microglial cell density and T1 intensity indices across all regions sampled. In combination with our previous report documenting a direct correlation between globus pallidus microglial density and cumulative Mn exposure (Gonzalez-Cuyar et al., 2013), this study provides further indirect evidence for the hypothesis that pre-clinical stage of Mn-induced neurotoxicity might be characterized by an initial inflammatory microglia response to Mn, ultimately progressing to astrocyte disruption and neuronal injury. This represents a testable, biologically plausible theory that can be confirmed in future studies.

Given the paramagnetic properties of Mn, it has been reasonably assumed the increased T1 basal ganglia signal would be associated with an increase in Mn tissue concentration. However, in this group there was no difference in tissue Mn concentration between the Mn-exposed and non-exposed groups, similar to previous studies in non-human primates (Olanow et al., 1996) and the case report by Yamada et al. (1986) where Mn tissue levels were normal following well-documented Mn exposures and clinical toxicity. It is important to note that MRI does not directly image Mn but rather its effects on the surrounding tissue (Kang et al., 1984; Cory et al., 1987). Therefore it is possible that Mn may have effluxed from the brain prior to autopsy, but the secondary tissue effects persist. Alternative causes of increased T1 signal include hemorrhage, HIV, melanin-, lipid-, and mineral-containing lesions (Ginat and Meyers, 2012). It is possible the increased T1 intensity indices may be from one of these other sources of T1 signal change; however, there has been no evidence of blood, melanin, or lipid accumulating lesions in Mn neurotoxicity. HIV infection is a potential concern in these mine workers as the prevalence of HIV is high in South Africa (Shisana, 2009), but there were no HIV pathologies identified in this cohort. Olanow et al. (1996) documented no difference in tissue Mn in their Mn-exposed animals but noted aluminum and Fe accumulation in the globus pallidus and substantia nigra pars reticularis. While we did not test for all paramagnetic metals (specifically aluminum), we found no differences in tissue metal levels for Mn, potassium, phosphorus, calcium, copper, zinc, lead, or magnesium between the exposed and non-exposed groups that would account for the differences in

Table 3
Mn and Fe metal data from Mn Mine workers and non-Mn mine workers ($n = 12$).

Metal	Region	Non-Mn mine workers ($n = 5$)	Mn Mine workers ($n = 7$)	p-Value
Mn (mean μg/g ± SD)	Caudate	0.100 ± 0.048	0.111 ± 0.046	0.943
	Globus Pallidus	0.154 ± 0.043	0.163 ± 0.033	0.811
	Putamen	0.118 ± 0.050	0.124 ± 0.045	0.897
Fe (mean μg/g ± SD)	Caudate	73.7 ± 36.0	61.8 ± 18.6	0.269
	Globus Pallidus	164.2 ± 37.5	131.4 ± 38.6	0.522
	Putamen	98.62 ± 55.5	83.5 ± 31.9	0.475
Mn/Fe ratio (mean ± SD)	Caudate	0.0017 ± 0.0014	0.0019 ± 0.0010	0.974
	Globus Pallidus	0.0010 ± 0.0004	0.0013 ± 0.0005	0.698
	Putamen	0.0015 ± 0.0011	0.0016 ± 0.0007	0.812

Multivariate generalized linear modeling compared differences between groups for each region adjusted for time from last Mn exposure to death.

intensity indices. Interestingly, we did find a trend toward lower tissue Fe concentrations in Mn-exposed miners, and Fe is a paramagnetic metal which shortens T1 (Zhang et al., 2009). The lower Fe concentrations could therefore lower the T1-weighted signal, thus underestimating the effects of Mn in the brains of exposed miners. Further complicating this measurement, brain Mn and Fe concentrations are interrelated as they are known to compete for the same metal transporter responsible for uptake into the brain (Zhang et al., 2009; Fitsanakis et al., 2010). Future studies will be needed to determine if the relative concentrations of Mn and Fe, or other metals, drives the signal characteristics and the resulting neurotoxicity.

The most important limitation of this study is the relatively small sample size that was used to evaluate ex vivo imaging in Mn mine workers. Nonetheless, this is by far the largest imaging-pathology study reported in humans. While we demonstrated similar T1 findings to previous in vivo imaging studies of Mn exposure (Criswell et al., 2012), we do not have in vivo imaging from this cohort for a direct comparison between imaging techniques. Further, we report on associations, but this paper lacks the evidence necessary to demonstrate a cause and effect relationship. The imaging studies and metal quantification have been also been performed at a single time point. We did adjust for the time from death to imaging within our analysis of intensity indices but we cannot directly measure the longitudinal effects of fixation or post-mortem processing of the brains. Finally, the cell density technique, while routinely used by pathologists, is not as precise as stereological counting. Future studies using a larger sample, with stereological counting could improve our ability to investigate relationships between pathologic outcomes, imaging, and exposure.

In conclusion, Mn mine workers demonstrated increased T1 basal ganglia intensity indices on ex vivo imaging when compared to non-Mn mine workers in all regions sampled. As with in vivo T1 imaging, the ex vivo intensity indices increased with cumulative Mn exposure. Caudate and putamen intensity indices were inversely associated with neuronal density but not with tissue Mn concentration. Ex vivo imaging provides a valid method to examine Mn neurotoxicity and a cost effective platform for developing and refining future in vivo imaging techniques. Future ex vivo studies with expanded exposure assessment, tissue Mn and Fe quantification, and stereology may ultimately lead to a better understanding of the mechanism of Mn neurotoxicity.

Conflict of interest statement

Dr. Gonzalez-Cuyar, Dr. Checkoway, Dr. Dills, Mr. Huang, Dr. Nelson, Dr. Shimony, and Dr. Sexias have nothing to disclose. Dr. Criswell reports grants from the National Institute of Environmental Health Sciences during the conduct of the study and participation as a site investigator for clinical trials sponsored by Adamas Pharmaceuticals, Auspex, Merz, Kyowa Hakko Kirin Pharma, Phytopharm, MERCK, Allergan, Teva, Solstice, and Civitas outside the submitted work. Dr. Racette reports grants from the National Institute of Environmental Health Sciences during the conduct of the study and participation as a site investigator for clinical trials sponsored by Allergan, Merz, US WoldMeds, LLC, Avid, Teva, AbbVie, Solstice, Adamas, Auspex, Kyowa Hakko Kirin Pharma, Inc. outside the submitted work. Dr. Simpson reports grants from National Institute of Environmental Health Sciences, USA, during the conduct of the study.

Transparency document

The Transparency document associated with this article can be found in the online version.

Acknowledgements

Funding sources for study: Grant Numbers: ES007033, K23 ES021444-01, K24ES017765-01A2, R21 ES017504-01, R01ES019277, P42ES004696, R01ES021488, and ICTS UL1RR024992.

References

Astafiev SV, Snyder AZ, Shulman GL, Corbetta M. Comment on "Modafinil shifts human locus coeruleus to low-tonic, high-phasic activity during functional MRI" and "Homeostatic sleep pressure and responses to sustained attention in the suprachiasmatic area". Science 2010;328:309. http://dx.doi.org/10.1126/science.1177200 author reply.

Augustinack JC, van der Kouwe AJ, Fischl B. Medial temporal cortices in ex vivo magnetic resonance imaging. J Comp Neurol 2013;521:4177–88. http://dx.doi.org/10.1002/cne.23432.

Baba Y, Lerch MM, Stark DD, Tanimoto A, Kreft BP, Zhao L, et al. Time after excision and temperature alter ex vivo tissue relaxation time measurements. J Magn Reson Imaging 1994;4:647–51. http://dx.doi.org/10.1002/jmri.1880040504.

Baltes C, Princz-Kranz F, Rudin M, Mueggler T. Detecting amyloid-beta plaques in Alzheimer's disease. Methods Mol Biol 2011;711:511–33. http://dx.doi.org/10.1007/978-1-61737-992-5_26.

Benjamini Y, Hochberg Y. Controlling the false discovery rate – a practical and powerful approach to multiple testing. J Roy Stat Soc B Met 1995;57:289–300.

Bowler RM, Nakagawa S, Drezgic M, Roels HA, Park RM, Diamond E, et al. Sequelae of fume exposure in confined space welding: a neurological and neuropsychological case series. Neurotoxicology 2007;28:298–311. http://dx.doi.org/10.1016/j.neuro.2006.11.001.

Butterworth RF, Spahr L, Fontaine S, Layrargues GP. Manganese toxicity, dopaminergic dysfunction and hepatic encephalopathy. Metab Brain Dis 1995;10:259–67. http://dx.doi.org/10.1007/bf02109357.

Canavan MM, Cobb W, Drnovsek B. Chronic manganese poisoning: report of a case with autopsy. Arch Neurol Psychiatr 1934;10:259–67.

Casamajor L. An unusual form of mineral poisoning affecting the nervous system: manganese. J Am Med Assoc 1913;60:646–9. http://dx.doi.org/10.1001/jama.1913.04340090008003.

Chang Y, Woo ST, Kim Y, Lee JJ, Song HJ, Lee HJ, et al. Pallidal index measured with three-dimensional T1-weighted gradient echo sequence is a good predictor of manganese exposure in welders. J Magn Reson Imaging 2010;31:1020–6. http://dx.doi.org/10.1002/jmri.22104.

Cory DA, Schwartzentruber DJ, Mock BH. Ingested manganese chloride as a contrast agent for magnetic resonance imaging. Magn Reson Imaging 1987;5:65–70. http://dx.doi.org/10.1016/0730-725x(87)90485-1.

Criswell SR, Perlmutter JS, Huang JL, Golchin N, Flores HP, Hobson A, et al. Basal ganglia intensity indices and diffusion weighted imaging in manganese-exposed welders. Occup Environ Med 2012;69:437–43. http://dx.doi.org/10.1136/oemed-2011-100119.

Dietz MC, Ihrig A, Wrazidlo W, Bader M, Jansen O, Triebig G. Results of magnetic resonance imaging in long-term manganese dioxide-exposed workers. Environ Res 2001;85:37–40. http://dx.doi.org/10.1006/enrs.2000.4068.

Eriksson H, Magiste K, Plantin LO, Fonnon F, Hedstöm KG, Theodorsson-Norheim E, et al. Effects of manganese oxide on monkeys as revealed by a combined neurochemical, histological and neurophysiological evaluation. Arch Toxicol 1987;61:46–52. http://dx.doi.org/10.1007/bf00324547.

Fitsanakis VA, Zhang N, Garcia S, Aschner M, Manganese. (Mn) and iron (Fe): interdependency of transport and regulation. Neurotox Res 2010;18:124–31. http://dx.doi.org/10.1007/s12640-009-9130-1.

Garbelli R, Zucca I, Milesi G, Mastropietro A, D'Incerti L, Tassi L, et al. Combined 7-T MRI and histopathologic study of normal and dysplastic samples from patients with TLE Neurology 2011;76:1177–85. http://dx.doi.org/10.1212/WNL.0b013e318212aae1.

Ginat DT, Meyers SP. Intracranial lesions with high signal intensity on T1-weighted MR images: differential diagnosis. Radiographics 2012;32:499–516. http://dx.doi.org/10.1148/rg.322105761.

Gonzalez-Cuyar LF, Nelson G, Criswell SR, Ho P, Lonzanida JA, Checkoway H, et al. Quantitative neuropathology associated with chronic manganese exposure in South African mine workers. Neurotoxicology 2014;45:260–6. http://dx.doi.org/10.1016/j.neuro.2013.12.008.

Guilarte TR, Chen MK, McGlothan JL, Verina T, Wong DF, Zhou Y, et al. Nigrostriatal dopamine system dysfunction and subtle motor deficits in manganese-exposed non-human primates. Exp Neurol 2006;202:381–90. http://dx.doi.org/10.1016/j.expneurol.2006.06.015.

Guilarte TR, Burton NC, McGlothan JL, Verina T, Zhou Y, Alexander M, et al. Impairment of nigrostriatal dopamine neurotransmission by manganese is mediated by pre-synaptic mechanism(s): implications to manganese-induced Parkinsonism. J Neurochem 2008;107:1236–47. http://dx.doi.org/10.1111/j.1471-4159.2008.05695.x.

Han JH, Chung YH, Park JD, Kim CY, Yang SO, Khang HS, et al. Recovery from welding-fume-exposure-induced MRI T1 signal intensities after cessation of welding-fume exposure in brains of cynomolgus monkeys. Inhal Toxicol 2008;20:1075–83. http://dx.doi.org/10.1080/08958370802116634.

Henriksen O, de Certaines JD, Spisni A, Cortsen M, Muller RN, Ring PB. In vivo field dependence of proton relaxation times in human brain, liver and skeletal muscle: a multicenter study. Magn Reson Imaging 1993;11:851–6. http://dx.doi.org/10.1016/0730-725x(93)90202-o.

Huang CC. Parkinsonism induced by chronic manganese intoxication – an experience in Taiwan. Chang Gung Med J 2007;30:385–95.
Kang YS, Gore JC, Armitage IM. Studies of factors affecting the design of NMR contrast agents: manganese in blood as a model system. Magn Reson Med 1984;1:396–409. http://dx.doi.org/10.1002/mmm.1910010310.
Kim Y, Kim KS, Yang JS, Park IJ, Kim E, Jin Y, et al. Increase in signal intensities on T1-weighted magnetic resonance images in asymptomatic manganese-exposed workers. Neurotoxicology 1999;20:901–7.
Maffeo E, Montuschi A, Stura G, Giordana MT. Chronic acquired hepatocerebral degeneration, pallidal T1 MRI hyperintensity and manganese in a series of cirrhotic patients. Neurol Sci 2014;35:523–30. http://dx.doi.org/10.1007/s10072-013-1458-x.
Nelson K, Golnick J, Korn T, Angle C. Manganese encephalopathy: utility of early magnetic resonance imaging. Br J Ind Med 1993;50:510–3. http://dx.doi.org/10.1136/oem.50.6.510.
Nelson G, Criswell SR, Zhang J, Murray J, Racette BA. Research capacity development in South African manganese mines to bridge exposure and neuropathologic outcomes. Neurotoxicology 2012;33:683–6. http://dx.doi.org/10.1016/j.neuro.2012.01.003.
Newland MC. Animal models of manganese's neurotoxicity. Neurotoxicology 1999;20:415–32.
Olanow CW, Good PF, Shinotoh H, Hewitt KA, Vingerhoets F, Snow BJ, et al. Manganese intoxication in the rhesus monkey: a clinical, imaging, pathologic, and biochemical study. Neurology 1996;46:492–8. http://dx.doi.org/10.1212/wnl.46.2.492.
Park RM, Bowler RM, Roels HA. Exposure–response relationship and risk assessment for cognitive deficits in early welding-induced manganism. J Occup Environ Med 2009;5:1125–36. http://dx.doi.org/10.1097/JOM.0b013e318bd8114.
Pujol A, Pujol J, Graus F, Rimola A, Peri J, Mercader JM, et al. Hyperintense globus pallidus on T1-weighted MRI in cirrhotic patients is associated with severity of liver failure. Neurology 1993;43:65–9.
Racette BA, Criswell SR, Lundin JI, Hobson A, Sexias N, Kotzbauer PT, et al. Increased risk of parkinsonism associated with welding exposure. Neurotoxicology 2012;33:1356–61. http://dx.doi.org/10.1016/j.neuro.2012.08.011.
Riddle A, Dean J, Buser JR, Gong X, Maire J, Chen K, et al. Histopathological correlates of magnetic resonance imaging-defined chronic perinatal white matter injury. Ann Neurol 2011;70:493–507. http://dx.doi.org/10.1002/ana.22501.
Rodier J. Manganese poisoning in Moroccan miners. Br J Ind Med 1955;12:21–35. http://dx.doi.org/10.1136/oem.12.1.21.
Salat DH, Lee SY, van der Kouwe AJ, Greve DN, Fischl B, Rosas HD. Age-associated alterations in cortical gray and white matter signal intensity and gray to white matter contrast. Neuroimage 2009;48:21–8. http://dx.doi.org/10.1016/j.neuroimage.2009.06.074.
Shisana O, Human Sciences Research Council, Centre for AIDS Development Research and Evaluation, South African Medical Research Council, National Institute for Communicable Diseases (South Africa). South African national HIV prevalence, incidence, behaviour and communication survey, 2008: a turning tide among teenagers. Cape Town: HSRC Press; 2009.
Spahr L, Butterworth RF, Fontaine S, Bui L, Therrien G, Milette PC, et al. Increased blood manganese in cirrhotic patients: relationship to pallidal magnetic resonance signal hyperintensity and neurological symptoms. Hepatology 1996;24:1116–20. http://dx.doi.org/10.1002/hep.510240523.
Tovi M, Ericsson A. Measurements of T1 and T2 over time in formalin-fixed human whole-brain specimens. Acta Radiol 1992;33:400–4. http://dx.doi.org/10.3109/02841859209172001.
Yamada M, Ohno S, Okayasu I, Okeda R, Hatakeyama S, Watanabe H, et al. Chronic manganese poisoning: a neuropathological study with determination of manganese distribution in the brain. Acta Neuropathol 1986;70:273–8. http://dx.doi.org/10.1007/bf00686083.
Yoo YC, Lee SK, Yang JY, In SW, Kim KW, Chung KH, et al. Organ distribution of heavy metals in autopsy material from normal Korean. J Health Sci 2002;48:186–94. http://dx.doi.org/10.1248/jhs.48.186.
Zhang N, Fitsanakis VA, Erikson KM, Aschner M, Avison MJ, Gore JC. A model for the analysis of competitive relaxation effects of manganese and iron in vivo. NMR Biomed 2009;22:391–404. http://dx.doi.org/10.1002/nbm.1348.